

# Ghost imaging in scattering media

Wenlin Gong, Pengli Zhang, Xia Shen, and Shensheng Han\*  
 Key Laboratory for Quantum Optics and Center for Cold Atom Physics,  
 Shanghai Institute of Optics and Fine Mechanics,  
 Chinese Academy of Sciences, Shanghai 201800, China  
 (Dated: October 12, 2021)

Ghost imaging with thermal light in scattering media is investigated. We demonstrated both theoretically and experimentally for the first time that the image with high quality can still be obtained in the scattering media by ghost imaging. The scattering effect on the qualities of the images obtained when the object is illuminated directly by the thermal light and ghost imaging is analyzed theoretically. Its potential applications are also discussed.

PACS numbers: 42.50.Ar, 42.68.Mj, 42.50.Dv, 42.62.Be, 42.30.Kq

## I. INTRODUCTION

Multiple scattering has a great effect on the qualities of images and the transmission of information. The information will be decayed and the images suffer reduced resolution and contrast because of multiple scattering. For example, the measurement of the laser radar [1], satellite communications [2], the propagation and imaging of light in the atmosphere [3], neutron imaging [4] and the imaging and diagnosis in life and medical science [5]. So the imaging in strong scattering media is always a great problem and presents a key challenge for the research of better imaging method and technique.

In clinic applications, the most common imaging modalities include ultrasound imaging, X-ray computed tomography(CT), and magnetic resonance imaging (MRI) [5, 6]. As the development of imaging technology, optical imaging is becoming an increasing interesting method for the imaging in biological tissue. By now most imaging methods are obtained by using the gating techniques. Such as confocal imaging, spatial filtering, optical coherence tomography (OCT), Mueller optical coherence tomography, Diffuse optical tomography (DOT), Photoacoustic tomography (PAT), Ultrasound-Modulated optical tomograph (UOT) and so on [6, 7, 8, 9, 10, 11, 12, 13, 14, 15]. Although the qualities of the images have a great increase by these techniques, there is still lots of problems which are difficult to be done. Because the imaging techniques in scattering media discussed above mainly are only the first-order effect of light field, detection and imaging are unseparated. When the information of the object is distorted by multiple scattering, and the information of both multiple scattering and the object is unknown, so we can not, in principle, obtain exactly the images destroyed by the multiple scattering, which leads to be impossible of the restoration of the qualities of images caused by multiple scattering.

The first two-photon imaging experiment with entan-

gled source was demonstrated by Pittman *et al.* in 1995 [16], which shew that we could obtain a nonlocal image by transmitting pairs of photons through a test and a reference path. Since 2002, the theories and experiments demonstrated that the ghost imaging could also be obtained with thermal light [17, 18, 19, 20, 21, 22]. And the fierce discussion on the essence of ghost imaging at one time [24, 25, 26]. Ghost imaging is considered as the effect of second-order correlation of light field and is caused by the undistinguishable relation of identical particles [23, 24, 26]. For the first time, detection and imaging are separated by ghost imaging. The test path and the reference path are used to detect the information from the object and imaging for the object, respectively. Recently we find that the qualities of ghost images are determined by both the reference path and test path [27]. Because multiple scattering only degrades the imaging quality in the test path, whereas there is no multiple scattering in the reference path. By correlation measurement, we may get a image with much better quality than the image obtained by detection in a single path.

## II. THEORY AND ANALYSIS

Schematic diagram for the light transmitting in a scattering media is shown in Fig. 1. In the theory of linear systems [29], the light field  $E(x)$  on the plane  $x$  is the convolution of the light field  $E(x_0)$  on the plane  $x_0$  and the impulse response function  $h(x, x_0)$ .

$$E(x) = \int dx_0 E(x_0) h(x, x_0). \quad (1)$$

For light transmission in scattering media, the light field on the position  $x$  is the linear superposition the incident light and the scattering light.

$$E(x) = \alpha \int dx_0 E(x_0) h_{in}(x, x_0) + \beta \int dx_0 E(x_0) h_{sca}(x, x_0), \quad (2)$$

---

\*Electronic address: sshan@mail.shcnc.ac.cn

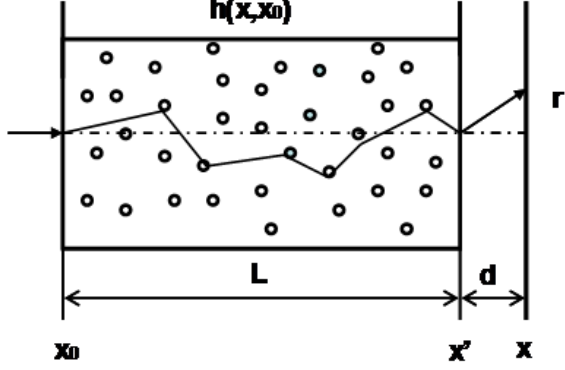


FIG. 1: Schematic diagram for the light transmitting in a scattering media.

$$|\alpha|^2 + |\beta|^2 = 1. \quad (3)$$

where  $h_{in}(x, x_0)$  is the impulse response function with no scattering media, and  $h_{sca}(x, x_0)$  is the impulse response function from the plane  $x_0$  to the plane  $x$  because of the interactions of multiple scattering, and  $\alpha, \beta$  are the probability amplitudes of the incident light and the scattering light, respectively. From Eqs. (1)-(3), we have

$$h(x, x_0) = \alpha h_{in}(x, x_0) + \beta h_{sca}(x, x_0). \quad (4)$$

The probability distribution function in scattering media is called point scattering function. The impulse response function  $h_{sca}(x, x_0)$  has close contact with the point scattering function which is Dirac delta function when there is no scattering media. However, in the scattering media, it is a spread function with a broadening length, and generally the point scattering function has two forms: Lorentzian-shaped and Gaussian-shaped distribution [39, 40]. In multiple scattering Mie theory[30, 31, 32], both of probability amplitudes  $\alpha, \beta$  are depending on the diameter size of the particle  $D$ , the wavelength of the incident light  $\lambda$ , the concentration of suspended particles  $w$  and the effective length of scattering media  $L$ . According to the experiments and theories [33, 34, 35, 36, 37, 38, 39, 40], we have

$$\alpha = \alpha(D, \lambda, w, L) \propto \frac{\lambda^{b_\alpha}}{D^{a_\alpha} w^{c_\alpha} L^{d_\alpha}}, \quad (5a)$$

$$\beta = \beta(D, \lambda, w, L) \propto \frac{D^{a_\beta} w^{c_\beta} L^{d_\beta}}{\lambda^{b_\beta}}, \quad (5b)$$

$$h_{sca}(x, x_0) \propto \int dx' P(x', x_0)_{L_A} h(x, x')_{(L+d)}, \quad (5c)$$

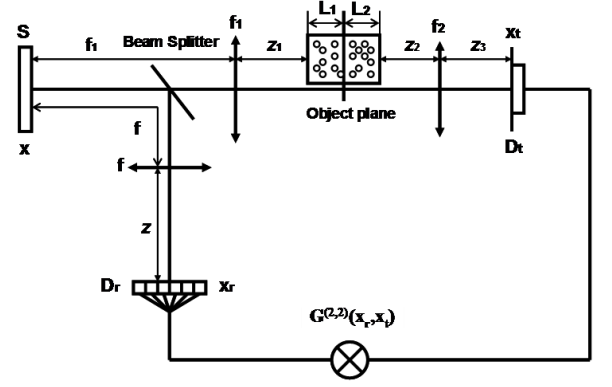


FIG. 2: Scheme for ghost imaging with thermal light in the scattering media.

$$P(x', x_0)_{L_A} = \left[ \frac{2}{\pi \Delta x_{L_A}^2} \right]^{1/4} \times \exp \left\{ - \left( \frac{x' - x_0}{\Delta x_{L_A}} \right)^2 \right\}, \quad (5d)$$

$$\Delta x_{L_A} \propto \frac{D^{a_x} w^{c_x} L_A^{d_x}}{\lambda^{b_x}}, \quad (5e)$$

$$\int |P(x', x_0)_{L_A}|^2 dx' = 1. \quad (5f)$$

where  $P(x', x_0)_{L_A}$  is point scattering probability amplitude.  $\Delta x_{L_A}$  is broadening length because of the interactions of multiple scattering, and it becomes wider with the increase of the scattering length. With the increase of the broadening length, the frequency spectrum of the optical transfer function becomes narrower, which is the main reason leading to the degradation of the quality of information transmission and images [37, 38]. We suppose point scattering function is Gaussian-shaped distribution without considering the absorption of scattering media. All the coefficients in Eq. (5) should be determined by specific experimental conditions.

The scheme for ghost imaging with thermal light in the scattering media is shown in Fig. 2. The light source  $S$ , first propagates through a beam splitter, then is divided into a test and a reference path. In the test path, the light propagates through a single lens of focal length  $f_1$ , the scattering media and then to the detector  $D_t$ . In the reference path, the light propagates through a single lens of focal length  $f$  then to an array of pixel detector  $D_r$ .

By optical coherence theory [17, 28], we can obtain the correlation function of intensity fluctuations between the detectors:

$$\Delta G^{(2,2)}(x_r, x_t) = \langle \Delta I_r(x_r) \Delta I_t(x_t) \rangle = |\Gamma(x_r, x_t)|^2, \quad (6a)$$

$$\Gamma(x_r, x_t) = \int dx_1 \int dx_2 G^{(1,1)}(x_1, x_2) h_r^*(x_r, x_1) \times h_t(x_t, x_2). \quad (6b)$$

where  $\Gamma(x_r, x_t)$  is the first-order cross-correlation function of two different points from the test and reference paths.

Suppose the light source is fully spatially incoherent, then

$$G^{(1,1)}(x_1, x_2) = I_0 \delta(x_1 - x_2). \quad (7)$$

where  $I_0$  is a constant, and  $\delta(x)$  is the Dirac delta function.

Under the paraxial and small angle approximation, and when the effective apertures of the lenses in the optical system are large enough, the impulse response function of the reference system is

$$h_r(x_r, x_1) \propto \exp \left\{ \frac{j\pi}{\lambda f} \left(1 - \frac{z}{f}\right) x_1^2 - \frac{2j\pi}{\lambda f} x_r x_1 \right\}. \quad (8)$$

And  $f_2, z_2 + L_2, z_3$  obey the Lens Law

$$\frac{1}{z_2 + L_2} + \frac{1}{z_3} = \frac{1}{f_2}. \quad (9)$$

when

$$\frac{f_1}{f} = \frac{z_2 + L_2}{z_3}. \quad (10)$$

The impulse response function of the test system is

$$\begin{aligned} h(x_t, x_2) \propto & \int dx' [\alpha_1 \exp \left\{ -\frac{2j\pi}{\lambda f_1} x' x_2 \right\} + \beta_1 \int dx'_2 \\ & \times P(x', x'_2)_{L_{1A}} \exp \left\{ -\frac{2j\pi}{\lambda f_1} x'_2 x_2 \right\}] t(x') C(x') \\ & \times \exp \left\{ \frac{j\pi}{\lambda f_1} \left(1 - \frac{z_1 + L_1}{f_1}\right) x_2^2 \right\} \end{aligned} \quad (11a)$$

$$\begin{aligned} C(x) = & [\alpha_2 \delta(x + \frac{f_1}{f} x_t) \exp \left\{ \frac{j\pi}{\lambda(L_2 + z_2)} x^2 \right\} + \beta_2 \\ & \times P(-\frac{f_1}{f} x_t, x)_{L_{2A}} \exp \left\{ \frac{j\pi}{\lambda(L_2 + z_2)} \left(\frac{f_1}{f} x_t\right)^2 \right\}] \end{aligned} \quad (11b)$$

Substituting Eqs. (7) and (9)-(11b) into Eq. (6b), we can get the intensity distribution in the test path

$$\begin{aligned} I(x_t) \propto & \int dx' \int dx'' t(x') t^*(x'') \{ |\alpha_1|^2 \delta(x' - x'') \\ & + 2P(x', x'')_{L_{1A}} \text{Re}[\alpha_1^* \beta_1] + |\beta_1|^2 \int dx'_2 \\ & \times P(x', x'_2)_{L_{1A}} P(x'', x'_2)_{L_{1A}} \} C(x') C^*(x''). \end{aligned} \quad (12)$$

Eq. (12) describes the images in the scattering media for the direct illumination of the thermal light. When

$$\frac{1 - \frac{z}{f}}{f} = \frac{1 - \frac{z_1 + L_1}{f_1}}{f_1}. \quad (13)$$

substituting Eqs. (7)-(11b) and (13) into Eq. (6), we can obtain the correlation function of intensity fluctuations

$$\begin{aligned} \Delta G^{(2)}(x_r, x_t) \propto & |\alpha_1 \alpha_2 C_1 + \alpha_1 \beta_2 C_2 \\ & + \beta_1 \alpha_2 C_3 + \beta_1 \beta_2 C_4|^2, \end{aligned} \quad (14a)$$

$$C_1 = \delta(x_r + x_t) t(-\frac{f_1}{f} x_t), \quad (14b)$$

$$C_2 = t(\frac{f_1}{f} x_r) P(-\frac{f_1}{f} x_t, \frac{f_1}{f} x_r)_{L_{2A}}, \quad (14c)$$

$$C_3 = t(-\frac{f_1}{f} x_t) P(-\frac{f_1}{f} x_t, \frac{f_1}{f} x_r)_{L_{1A}}, \quad (14d)$$

$$C_4 = \int dx' t(x') P(x', \frac{f_1}{f} x_r)_{L_{1A}} P(-\frac{f_1}{f} x_t, x')_{L_{2A}}. \quad (14e)$$

The ghost imaging in the scattering media is described by the Eqs. (14a)-(14e). And it is a image with high quality for  $C_1$  and  $C_2$ , which implies we can still get a image with high quality by ghost imaging in the scattering media.

From Eqs. (14a)-(14e), if the test detector is an array of pixel detector, and  $x_t = -x_r$ , after some calculation, then

$$\begin{aligned} \Delta G^{(2)}(x_r, -x_r) \propto & \left| \left\{ \alpha_1 \alpha_2 + \alpha_1 \beta_2 \left[ \frac{2}{\pi \Delta x_{L_{2A}}^2} \right]^{1/4} \right. \right. \\ & \left. \left. + \beta_1 \alpha_2 \left[ \frac{2}{\pi \Delta x_{L_{1A}}^2} \right]^{1/4} \right\} t\left(\frac{f_1}{f} x_r\right) + \beta_1 \beta_2 C_4 \right|^2. \end{aligned} \quad (15)$$

if the test detector is a bucket detector, then

$$\begin{aligned} \Delta G^{(2)}(x_r) \propto & \int dx_t |\alpha_1 \alpha_2 C_1 + \alpha_1 \beta_2 C_2 \\ & + \beta_1 \alpha_2 C_3 + \beta_1 \beta_2 C_4|^2. \end{aligned} \quad (16)$$

Eqs. (15) and (16) represent ghost imaging when the test detector is an array of pixel detector or a bucket detector, respectively. From Eqs. (15), if  $\beta_1 = 0$  (namely  $L_1 = 0$ ) or  $\beta_2 = 0$  (namely  $L_2 = 0$ ), it is clear to find that we can still obtain a image with high quality by ghost imaging in the scattering media. if  $\beta_1 \neq 0$  and  $\beta_2 \neq 0$  and as the increase of  $\beta_1$  and  $\beta_2$ , the qualities of ghost images will reduce, and the term including  $C_4$  is the main reason leading to the degradation of the qualities of the images.

For  $L_1 = 0$ , there is only multiple scattering between the object plane and the test detector, then we have  $|\alpha_1| = 1, \beta_1 = 0$ . By Eq. (12), the intensity distribution in the test path is

$$I_t(x_t) \propto (|\alpha_2|^2 + 2C_{5t}) \left| t(-\frac{f_1}{f} x_t) \right|^2 + C_{6t} |\beta_2|^2, \quad (17a)$$

$$C_{5t} = \left[ \frac{2}{\pi \Delta x_{L_{2A}}^2} \right]^{1/4} \text{Re}[\alpha_2^* \beta_2], \quad (17b)$$

$$\begin{aligned} C_{6t} &= \int dx' |t(x')|^2 \left| P\left(-\frac{f_1}{f} x_t, x'\right)_{L_{2A}} \right|^2 \\ &= \left[ \frac{2}{\pi \Delta x_{L_{2A}}^2} \right]^{1/2} \int dx' |t(x')|^2 \\ &\quad \times \exp \left\{ -\frac{2}{\Delta x_{L_{2A}}^2} \left(x' + \frac{f_1}{f} x_t\right)^2 \right\}. \end{aligned} \quad (17c)$$

the last term in Eq. (17a) is the main reason leading to the decrease of the quality of the image when there is multiple scattering between the object plane and the detector. With the increase of  $\beta_2$  (and the decrease of the probability amplitude  $\alpha_2$ ), the quality of the image will be further degraded.

Form Eq. (15), when the test detector is an array of pixel detector, after some calculation, then

$$\begin{aligned} \Delta G^{(2)}(x_r, -x_r) &\propto \left| \alpha_2 + \beta_2 \left[ \frac{2}{\pi \Delta x_{L_{2A}}^2} \right]^{1/4} \right|^2 \\ &\quad \times \left| t\left(\frac{f_1}{f} x_r\right) \right|^2. \end{aligned} \quad (18)$$

If the test detector is a bucket detector, By Eq. (16), then

$$\Delta G^{(2)}(x_r) \propto (|\alpha_2|^2 + 2C_5 + C_6 |\beta_2|^2) \left| t\left(\frac{f_1}{f} x_r\right) \right|^2, \quad (19a)$$

$$C_5 = \left[ \frac{2}{\pi \Delta x_{L_{2A}}^2} \right]^{1/4} \text{Re}[\alpha_2^* \beta_2], \quad (19b)$$

$$C_6 = \int dx_t \left| P\left(-\frac{f_1}{f} x_t, \frac{f_1}{f} x_r\right)_{L_{2A}} \right|^2 \sim 1. \quad (19c)$$

from Eqs. (18)-(19c), we find that whether the test detector is an array of pixel detector or a bucket detector, the qualities of ghost images can be obtained even though there is multiple scattering between the object plane and the test detector.

For  $L_2 = 0$ , there is only multiple scattering between the source and the object plane, then we can gain  $|\alpha_2| = 1, \beta_2 = 0$ . By Eq. (12), the intensity distribution in the test path is

$$I_t(x_t) \propto (|\alpha_1|^2 + 2C_{7t} + C_{8t} |\beta_1|^2) \left| t\left(-\frac{f_1}{f} x_t\right) \right|^2, \quad (20a)$$

$$C_{7t} = \left[ \frac{2}{\pi \Delta x_{L_{1A}}^2} \right]^{1/4} \text{Re}[\alpha_1^* \beta_1], \quad (20b)$$

$$C_{8t} = \int dx'_2 \left| P\left(-\frac{f_1}{f} x_t, x'_2\right)_{L_{1A}} \right|^2 \sim 1. \quad (20c)$$

From Eqs. (20a)-(20c), we find that the multiple scattering between the source and the object plane has no effect on the quality of the image.

From Eq. (15), when the test detector is an array of pixel detector, after some calculation, then

$$\begin{aligned} \Delta G^{(2)}(x_r, -x_r) &\propto \left| \alpha_1 + \beta_1 \left[ \frac{2}{\pi \Delta x_{L_{1A}}^2} \right]^{1/4} \right|^2 \\ &\quad \times \left| t\left(\frac{f_1}{f} x_r\right) \right|^2. \end{aligned} \quad (21)$$

which reveals that we can still obtain a image with high quality when the test detector is an array of pixel detector even if there is multiple scattering between the source and the object plane.

If the test detector is a bucket detector, By Eq. (16), then

$$\Delta G^{(2)}(x_r) \propto (|\alpha_1|^2 + 2C_7) \left| t\left(\frac{f_1}{f} x_r\right) \right|^2 + C_8 |\beta_1|^2, \quad (22a)$$

$$C_{7t} = \left[ \frac{2}{\pi \Delta x_{L_{1A}}^2} \right]^{1/4} \text{Re}[\alpha_1^* \beta_1], \quad (22b)$$

$$\begin{aligned} C_8 &= \int dx_t \left| t\left(-\frac{f_1}{f} x_t\right) P\left(-\frac{f_1}{f} x_t, \frac{f_1}{f} x_r\right)_{L_{1A}} \right|^2 \\ &= \left[ \frac{2}{\pi \Delta x_{L_{1A}}^2} \right]^{1/2} \int dx_t \left| t\left(-\frac{f_1}{f} x_t\right) \right|^2 \\ &\quad \times \exp \left\{ -\frac{2f_1^2}{\Delta x_{L_{1A}}^2 f^2} (x_t + x_r)^2 \right\}. \end{aligned} \quad (22c)$$

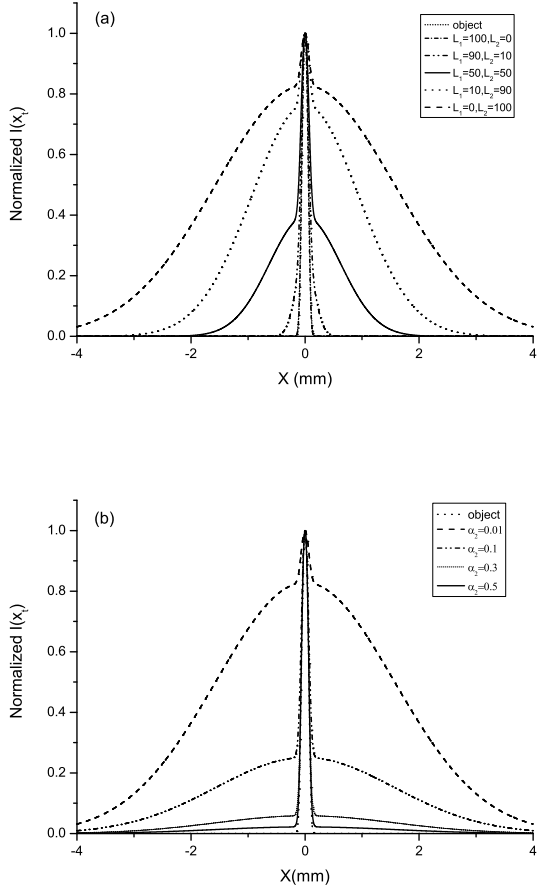
where  $C_8$  is the main factor leading to the decrease of the qualities of ghost images.  $f_1 > f$  is helpful to improve the quality of the image.

The second-order degree of coherence  $g^{(2)}(x_1, x_2)$  at the positions  $x_1$  and  $x_2$  can be defined as follows

$$g^{(2)}(x_1, x_2) = \frac{\langle I_1 \cdot I_2 \rangle}{\langle I_1 \rangle \langle I_2 \rangle} = 1 + \frac{\langle \Delta I_1 \cdot \Delta I_2 \rangle}{\langle I_1 \rangle \langle I_2 \rangle}. \quad (23)$$

for ghost imaging, The second-order degree of coherence  $g^{(2)}(x_{t1}, x_{t2})$  obtained only by the correlation measurement in the test path reveals the characteristic of the source, whereas  $g^{(2)}(x_r, x_t)$  describes the correlation between two paths. And the degradation of  $g^{(2)}(x_r, x_t)$  will lead to the decay of intensity fluctuations, which has a great effect on the visibility of ghost images.

Figs. 3-7 present numerical results of imaging a single slit in scattering media based on Eqs. (12) and (15)-(16) (in which we take  $\lambda=650\text{nm}$ ,  $f_1=400\text{mm}$ ,  $f=250\text{mm}$ , the single slit width  $a=0.2\text{mm}$ ). From Fig. 3(a), as the increase of  $L_2$ , the qualities of the images will decrease obviously when the object is illuminated directly by the thermal light. The quality of the image also degrade rapidly with the increase of the broadening length  $\Delta x_2$  and the



decrease of the probability amplitude  $\alpha_2$  when the object is fixed in the position of  $L_1=0\text{mm}$ ,  $L_2=100\text{mm}$  (Fig. 3(b), (c)), which accord with the results described by the Eqs (17a)-(17c).

Fig. 4 shows the numerical results when the position of the object in the scattering media is shifted. By Fig. 4(a), we can find that if the test detector is an array of pixel detector, multiple scattering has no effect on the qualities of ghost images when there is only multiple scattering either between the object plane and the test detector or between the object plane and the source. As the object is fixed closing to the middle of scattering media, the qualities of ghost images will decay. However, if the test detector is a bucket detector, the qualities of ghost images will decrease sharply with the degradation of  $L_1$ , which is opposite absolutely to imaging when the object is illuminated directly by the thermal light (Fig. 3(a)).

In Fig. 5, We give the comparison of the qualities of images between imaging by the direct illumination of the thermal light and ghost imaging when the object is fixed in the middle of scattering media. It is easy to find that we can only obtain the same image with low quality as imaging by the direct illumination of the thermal light when the test detector is a bucket detector by ghost imaging. But a image with high quality can still be

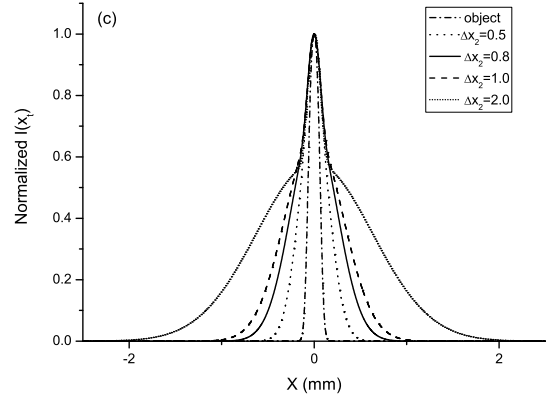
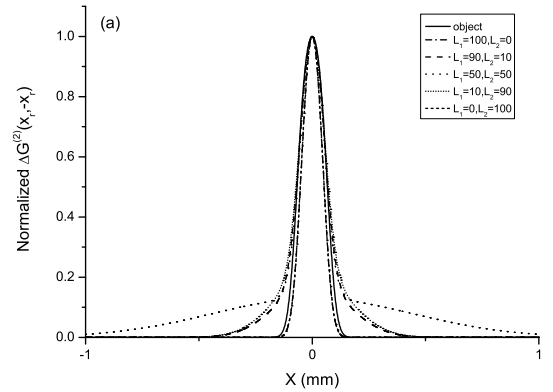


FIG. 3: Factors which have the effect on the qualities of the images when the object is illuminated directly by the thermal light. (a). Images of a single slit at different positions in the scattering media; (b). Images of a single slit for different probability amplitude  $\alpha_2$  when  $L_1=0\text{mm}$ ,  $L_2=100\text{mm}$  and the broadening length  $\Delta x_2=5.0$ ; and (c). Images of a single slit for different probability amplitude  $\Delta x_2$  when  $L_1=0\text{mm}$ ,  $L_2=100\text{mm}$  and the broadening length  $\alpha_2=0.05$ .



gained if the test detector is an array of pixel detector.

Results shown in Fig. 6 reveals that the qualities of ghost images will reduce obviously as the degradation of the probability amplitude  $\alpha_1$  and  $\alpha_2$ . And the object is still fixed in the middle of scattering media.

In order to improve the qualities of ghost images further, we investigate a new method to the effect on the qualities of ghost images by using a circular aperture gating to change the transverse coherent length near the scattering media in Fig. 7, which is different from the method to change the transverse size of the source. But when the space interval  $\Delta s$  is greater than the characteristic scale of the object, the diffraction will emerge.

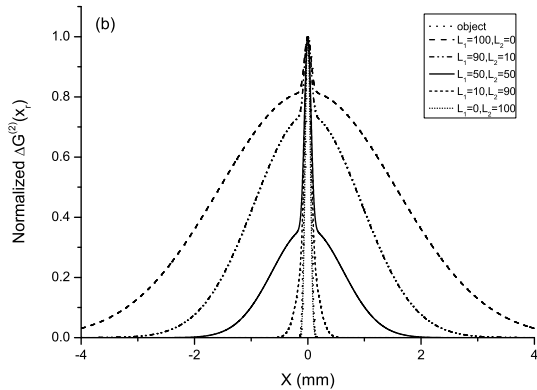


FIG. 4: Relationship between the qualities of ghost images and the position of the object in scattering media. (a). the test detector is an array of pixel detector; and (b). the test detector is a bucket detector.

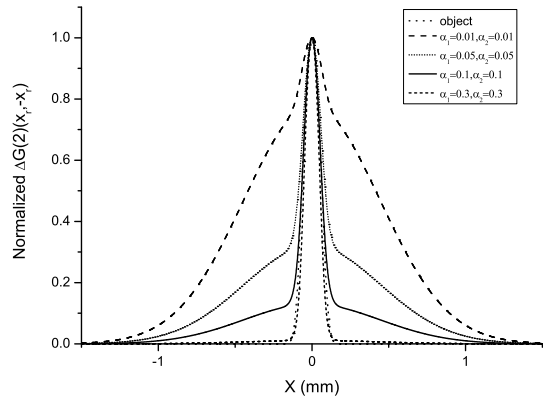


FIG. 6: Dependence of probability amplitude  $\alpha_2$  on the qualities of ghost images when  $L_1=50\text{mm}$ ,  $L_2=50\text{mm}$  and the broadening length  $\Delta x_1=2.0$ ,  $\Delta x_2=2.0$ .

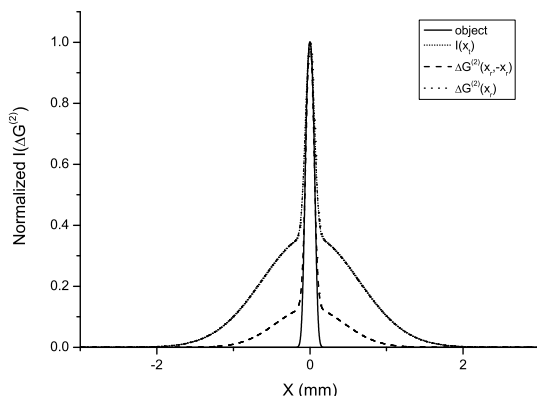


FIG. 5: Comparison between imaging by the direct illumination of the thermal light and ghost imaging when  $L_1=50\text{mm}$ ,  $L_2=50\text{mm}$ , the broadening length  $\Delta x_1=2.0$ ,  $\Delta x_2=2.0$  and  $\alpha_1=0.1$ ,  $\alpha_2=0.1$ .

### III. EXPERIMENT

In the experiments, we prepare a suspension liquid which is composed by emulsion polymerization particles with particle diameter  $D=3.26\mu\text{m}$  and the solution  $\text{NaCl}$  with the density  $\rho=1.19\text{ g/cm}^3$ . The vessel used to put the suspension liquid is designed as  $40\text{mm}\times 40\text{mm}\times 20\text{mm}$ . The liquid can be considered as strong multiple scattering media. And we take  $\lambda=650\text{nm}$ ,  $f_1=400\text{mm}$ ,  $f=250\text{mm}$ ,  $z=211\text{mm}$ ,  $z_1=300\text{mm}$ ,  $z_2=390\text{mm}$ ,  $z_3=243.8\text{mm}$ . The minimum characteristic scale of the object (**‘zhong’** ring) is  $60\mu\text{m}$  and the diameter of the ring is  $1.6\text{mm}$ . And the detectors in both paths are arrays of pixel detectors.

Images shown in Fig. 8 (1) and (2) were the experimental results of the object (**‘zhong’** ring) by direct illu-

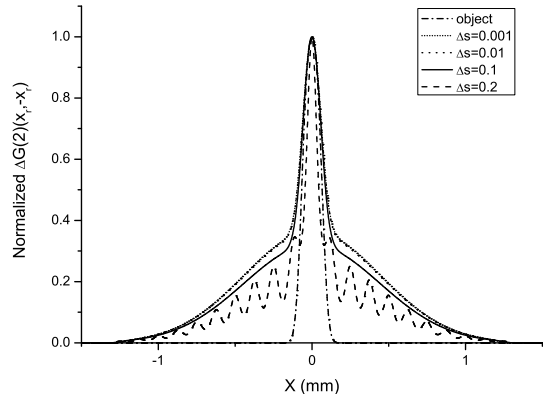


FIG. 7: The effect of the space interval  $\Delta s$  on the qualities of ghost images when a circular aperture gating with different space interval  $\Delta s$  is fixed on the plane  $x_0$ .  $L_1=50\text{mm}$ ,  $L_2=50\text{mm}$ , the broadening length  $\Delta x_1=2.0$ ,  $\Delta x_2=2.0$  and  $\alpha_1=0.1$ ,  $\alpha_2=0.1$ .

mination and ghost imaging when the object was fixed at different positions in the scattering media, respectively. From Fig. 8, when the object is illuminated directly by the thermal light, the qualities of images will reduce as the increase of the length  $L_2$  of scattering media. However, when there is only strong multiple scattering between the object plane and the source or between the object plane and the detector  $D_t$ , we can both obtain ghost images with high qualities. If the object is fixed in the middle of the scattering media, the visibility of ghost images will reduce, but the resolution doesn't degrade. All discussed above accord with the theoretical results described by the Eqs. (1).

In Fig. 9, we demonstrated experimentally that the effect of the concentration of scattering media or the co-

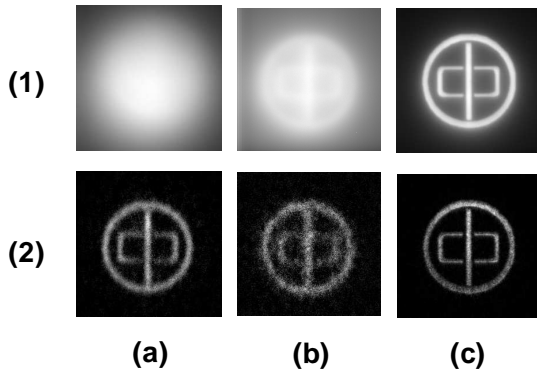


FIG. 8: Images of the aperture ('zhong' ring) when the object is fixed in different position of the scattering media. (a).  $L_1=0\text{mm}$ ,  $L_2=40\text{mm}$ ; (b).  $L_1=20\text{mm}$ ,  $L_2=20\text{mm}$ ; and (c).  $L_1=40\text{mm}$ ,  $L_2=0\text{mm}$ . (1). when the object was illuminated directly by thermal light; (2). ghost imaging.

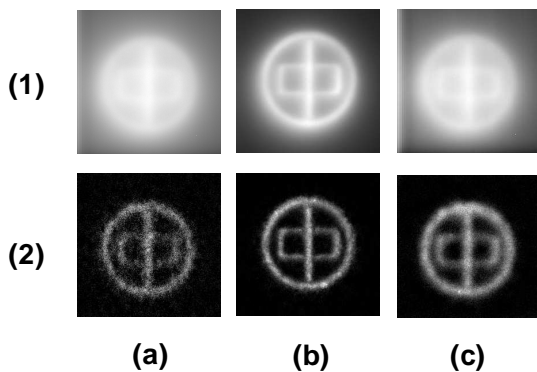


FIG. 9: Effect of the concentration of scattering media and the coherent length located at the object plane on ghost imaging. (a).  $L_c=40.6\mu\text{m}$ , 6 drops; (b).  $L_c=40.6\mu\text{m}$ , 3 drops; and (c).  $L_c=192.5\mu\text{m}$ , 6 drops. (1). when the object was illuminated directly by thermal light; (2). ghost imaging.

herent length located at the object plane on ghost imaging when the object is fixed in the middle of scattering media. The visibility of ghost images will reduce with the increase of the concentration of scattering media. When the coherent length located at the object plane becomes long, the visibility of ghost images will improve. However, the resolution will degrade.

Carves shown in Figs. 10 and 11 are the effect of concentration of emulsion polymerization particles on  $g^{(2)}$  when  $L_1=40\text{mm}$  and  $L_2=0\text{mm}$  and when  $L_1=20\text{mm}$  and  $L_2=20\text{mm}$  without the object, respectively. We can find that  $g^{(2)}(x_{t1}, x_{t2})$  and  $g^{(2)}(x_r, x_t)$  decay sharply with the increase of concentration of emulsion polymerization particles. When there is two drops emulsion polymerization particles put into the solution  $\text{NaCl}$ , the cross-correlation coefficient will be lower than 1.10.

When there are five drops emulsion polymerization

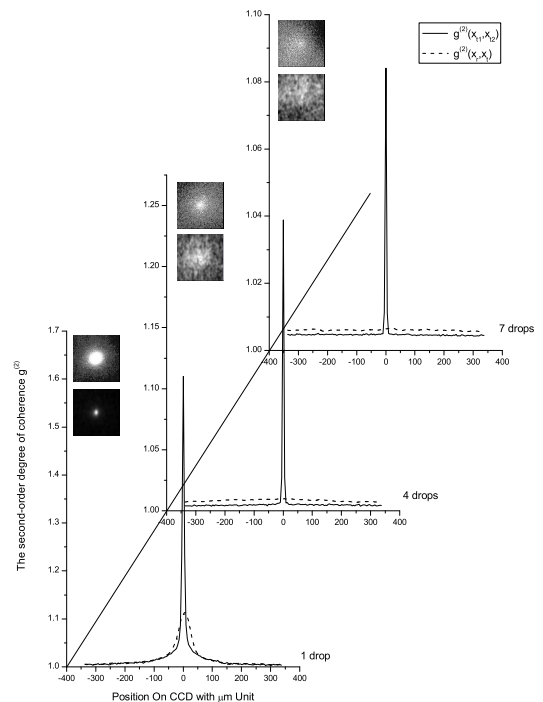
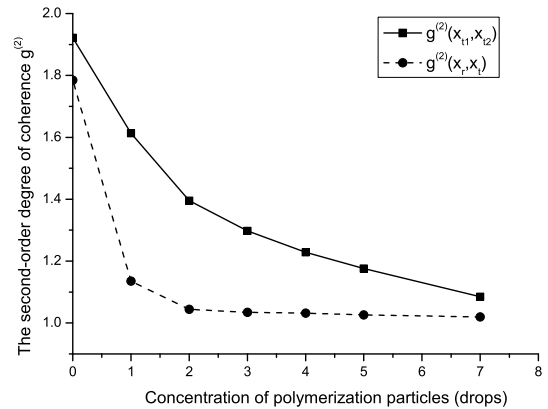


FIG. 10: The effect of concentration of emulsion polymerization particles on  $g^{(2)}$  when  $L_1=40\text{mm}$  and  $L_2=0\text{mm}$  without the object.

particles put into the solution  $\text{NaCl}$ , the intensity distribution on the detector  $D_r$  is heterogenous because there is no multiple scattering. However, we can find the homogeneous intensity distribution on the detector  $D_t$  (in Fig. 12).

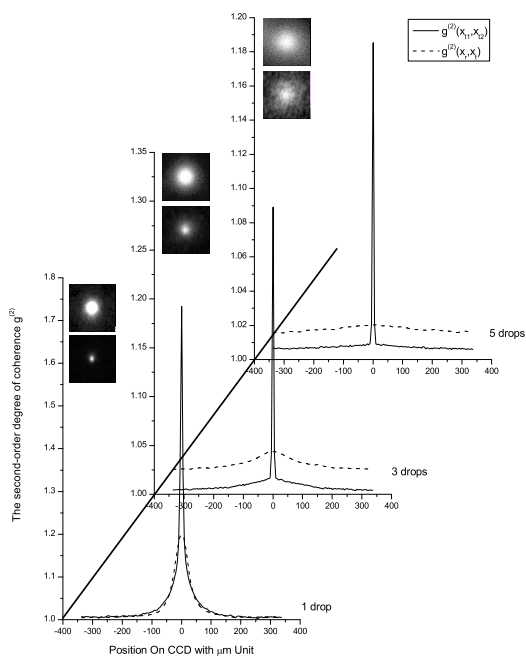
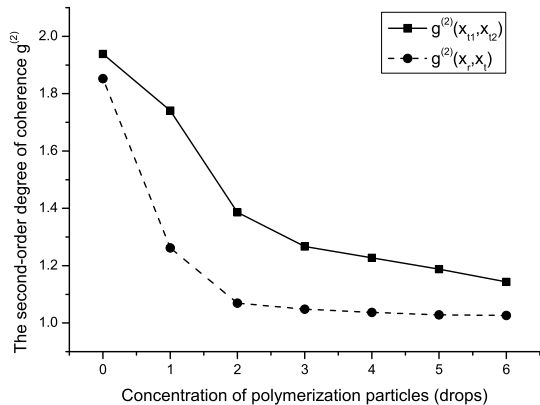


FIG. 11: The effect of concentration of emulsion polymerization particles on  $g^{(2)}$  when  $L_1=20\text{mm}$  and  $L_2=20\text{mm}$  without the object.

#### IV. DISCUSSION AND INCLUSION

When the object is illuminated directly by thermal light, multiple scattering between the object plane and the detector  $D_t$  is the main reason leading to the degradation of the qualities of images (Fig. 3). In scattering media, different from images obtained by the first-order correlation of light field, ghost imaging causes the separation of detection and imaging. Even if the information from the object is distorted by multiple scattering, there is no effect on ghost imaging. Because multiple scattering destroys the correlation of the light field, the

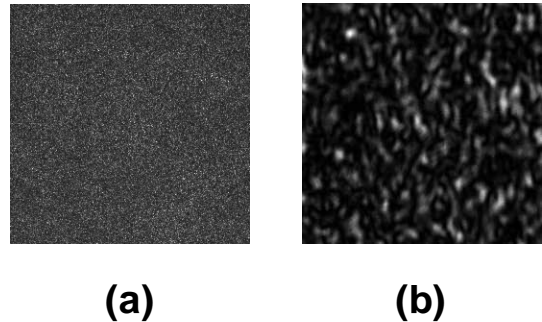


FIG. 12: Images from a single frame speckle distribution when  $L_1=20\text{mm}$  and  $L_2=20\text{mm}$  without the object and there are five drops emulsion polymerization particles put into the solution  $NaCl$ , (a). from the CCD camera  $D_t$ , (b). from the CCD camera  $D_r$ .

visibility of ghost images is degraded but the resolutions doesn't degrade. However, the visibility of ghost images can be enhanced by means of the decrease of the resolution [41, 42, 43, 44]. The experimental result in Fig. 9 (c) also demonstrated that. Transmission information of the light on the object plane (namely  $\alpha_1$ ) has a great effect on the visibility of ghost images. Because multiple scattering leads to the decay of the correlation between the test and reference paths with the decrease of Transmission information of the light (Figs 8 and 9). The higher the Transmission information is, the better visibility the ghost image has. When there is no multiple scattering between the object plane and the source, then ballistic component of the light on the object plane is equal to 1, so we can always obtain a ghost image with high quality whether there is multiple scattering between the object plane and the detector  $D_t$ . Otherwise, because the ballistic component of the light is impossible to be 0, we can always see the shapes of the object (Figs. 3(b) and 6). The degradation of the qualities of the images is provoked by the decay of visibility in scattering media, which is different absolutely from the low resolution caused by diffraction-limited. When the object is fixed in the middle of the scattering media, as shown in Fig. 11, even if the second-order degree of coherence  $g^{(2)}$  is very low, we can obtain a ghost image with much better quality than the image gained when the object is illuminated directly by thermal light. By the characteristics of ghost imaging, the qualities of ghost images does not depend on the intensity of the light but on the intensity fluctuations. As the multiple scattering increased, the intensity fluctuations will reduce (Figs 10 and 11), which leads to the degradation of the visibility of the image. The expression in the Eq. (15) can explain basically the experimental results and the fact discussed above, which shows that the results described by the Eq. (15) are reasonable for the description of ghost imaging in scattering media. However, when the test detector is



a bucket detector, the qualities of ghost images depend on the multiple scattering between the object plane and the source, which is opposite to imaging by the direct illumination of the thermal light (Fig. 3(a)). By the results in Fig. 8 (a) and (c), maybe we can also obtain a ghost image with high visibility by means of eliminating the multiple scattering between the object plane and the source or between the object plane and the detector  $D_t$ . One is like the technique of DOT. Firstly we obtain an improved image by iterative recovery method of DOT from a single frame of image collected by the detector  $D_t$ , then we will get a ghost image with improved visibility by the correlation measurement of intensity fluctuations between the detector  $D_r$  and the improved images. The other is that we get the intensity distribution on the object plane by the measurement to transmission and reflection coefficients, then do the correlation measurement of the intensity fluctuations between the detector  $D_t$  and intensity distribution obtained by numerical simulation. The method discussed in Fig. 7 can improve the visibility of ghost images to some extent. Generally speaking, by ghost imaging method, we can always obtain an image with much better quality on the base of the image obtained by a novel conventional imaging technique with thermal light. For entangled source, because of the entanglement characteristic of the two photons, maybe we can also improve the visibility of ghost images. Based on the effect of photon bunching, and the new source with high  $g^{(2)}$  can be obtained, the visibility of ghost images may also be enhanced obviously.

In medical science, in order to avoid ionizing radiation of X-ray, optical photons provides nonionizing and safe radiation for medical applications. Recently there has been increasing interest in the field of the imaging, test and diagnosis of the biological tissues with the infrared

and the near infrared light [6, 11, 15]. Because the near infrared light around 700-nm wavelength can penetrate several centimeters into biological tissue [15]. But several factors still limit the imaging quality. Because most biological tissues are characterized by strong optical scattering and hence are referred to as scattering media or turbid media. The images suffer reduced resolution and contrast due to multiple scattering, which leads to a low efficiency and accuracy of diagnosis and a difficulty of analysis in medical science. So the diffusion-like behavior of light in biological tissue presents a key challenge for optical imaging. The ghost imaging discussed here may solve the problems about the low quality of the imaging in biological tissues.

In conclusion, for the first time, detection and imaging of the object information are separated by ghost imaging, which provides a new way for imaging in scattering media. we have demonstrated experimentally and theoretically for the first time that the images with high qualities in a scattering media can still be obtained for ghost imaging when the test detector is an array of pixel detector and there is only multiple scattering between the object plane and the source or between the object plane and the detector. When the object is fixed in the middle of scattering media, we can also gain ghost images with much better qualities than the images obtained when the object is illuminated directly by the thermal light. The probability amplitudes of the incident light  $\alpha_1$  and  $\alpha_2$  have a great effect on the visibility of ghost images. These results will be very useful for the imaging and diagnosis in medical science.

The work was partly supported by the Hi-Tech Research and Development Program of China, Project No. 2006AA12Z115, and Shanghai Fundamental Research Project, Project No. 06JC14069.

- 
- [1] G. W. Kamerman, Proc. SPIE, **4377**, 126-131 (2001).
  - [2] H. G. Booker, and D. C. Miller, Journal of Atmospheric and Terrestrial Physics, **42**, 3 (1980).
  - [3] T. S. McKechnie, J. Opt. Soc. Am. A, **8**,2 (1991).
  - [4] Raine D. A. , and Brenizer J. S. Materials evaluation, **55**, 1174 (1997).
  - [5] K. P. Maher, J. F. Malone, and Brain Chance, Contemporary Physics, **38**, 131 (1997).
  - [6] Lihong V. Wang and Hsin-i Wu, Biomedical optics: principle and imaging, (2007).
  - [7] A. P. Gibson, J. C. Hebden and S. R. Arridge, Phys. Med. Biol. **50** R1-R43 (2005).
  - [8] A. Yodh, and B. Chance, Phys. Today, **48**, 34 (1995).
  - [9] S. R. Arridge, M. Cope, and D. T. Depty, Phys. Med. Biol. **37**, 1531 (1992).
  - [10] S. R. Arridge, Topical Review, R41-93 (1999).
  - [11] Sachin V. patwardhan, and Joseph P. Culver, J. Biomed. Opt. **13**(1), 011009 (2008).
  - [12] J. C. Hebden, S. R. Arridge, M. Cope, and D. T. Depty, Phys. Med. Biol. **42**, 825 (1997).
  - [13] B. Chance and R. R. Alfano, Proc. SPIE, 2389 (1995).
  - [14] M. Laubscher, M. Ducros, B. Karamata, Opt. Exp. **10**, 9 (2002)
  - [15] Brian C. Wilson, Eva M. Sevick, Michael S. Patterson, and Britton Chance, Proceedings of the IEEE. **80**, 6 (1992).
  - [16] T. B. Pittman, Y. H. Shih, D. V. Strekalov, and A. V. Sergienko, Phys. Rev. A. **52**. R3429 (1995).
  - [17] J. Cheng and S. Han, Phys. Rev. Lett. **92**. 093903 (2004).
  - [18] A. Gatti, E. Brambilla, M. Bache, and L. A. Lugiato, Phys. Rev. A. **70**. 013802 (2004).
  - [19] A. Gatti, E. Brambilla, M. Bache, and L. A. Lugiato, Phys. Rev. Lett. **93**. 093602 (2004).
  - [20] A. Valencia, G. Scarcelli, M. D'Angelo, and Y. Shih, Phys. Rev. Lett. **94**. 063601 (2005).
  - [21] R. S. Bennink, S. J. Bentley, and R. W. Boyd, Phys. Rev. Lett. **89**. 113601 (2002).
  - [22] L. Basano and P. Ottonello, Appl. Phys.Lett. **89**, 091109 (2006).
  - [23] Minghui Zhang, Qing Wei, and Shensheng Han, Phys. Lett. A. **366**, 569-574 (2007).
  - [24] G. Scarcelli, V. Berardi and Y. Shih, Phys. Rev. Lett.

- 96**, 063602 (2006).
- [25] A. Gatti, M. Bondani, L. A. Lugiato, M. G. A. Pairs, and C. Fabre, *Phys. Rev. Lett.* **98**, 039301 (2007).
- [26] G. Scarcelli, V. Berardi and Y. Shih, *Phys. Rev. Lett.* **98**, 039302 (2007).
- [27] Pengli Zhang, Wenlin Gong, Xia Shen, and Shensheng Han, arXiv. Quantum-ph/0804.0575 (2008).
- [28] R. J. Glauber, *Phys. Rev.* **130**, 2529 (1963).
- [29] J. W. Goodman, *Introduction to Fourier optics* (1976).
- [30] G. Mie, *Ann. Phys.* **330**, 377 (1908).
- [31] D. Toubanc, *Appl. Opt.* **35**, 3270 (1996).
- [32] S. K. Sharma, and A. K. Roy, *J. Quant. Spectrosc. Radiat. Transfer.* **64**, 327 (2000).
- [33] Jessica C. Ramella-Roman, Scott A. Prael, and Steven L. Jacques, *Opt. Exp.* **13**, 25 (2005).
- [34] Milun J. Rakovic and George W. Kattawar, *Appl. opt.* **37**, 15 (1999).
- [35] A. A. M. Mustafa and Daphne F. Jackson, *Phys. Med. Biol.* **26**, 461 (1981).
- [36] J. S. Faulkner and Eva A. Horvath, *Phys. Rev. B.* **44**, 8467 (1991).
- [37] W. H. Wells, *J. Opt. Soc. Am.* **59**, 6 (1969).
- [38] H. T. Yura, *Appl. opt.* **10**, 1 (1971).
- [39] Rene Hassanein, Eberhard Lehmann, and Peter Vontobel, *Nucl. Ins. Meth. Phys. Res. A.* **542**, 353 (2005).
- [40] P. N. Segre and P. N. Pusey, *Phys. Rev. Lett.* **77**, 4 (1996).
- [41] Shen Xia, Bai Yan-Feng, and Han Shen-Sheng, *Chin. Phys. Lett.* **25**, 11 (2007).
- [42] Y. Cai and S. Zhu, *Opt. Lett.* **29**, 2716 (2004).
- [43] Y. Cai and S. Zhu, *Opt. Lett.* **30**, 388 (2005).
- [44] A. Gatti, M. Bache, E. Brambilla, and L. A. Lugiato, *J. Mod. Opt.* **53**, 739 (2006).